

Article

Low-Frequency Noise Behavior of AlGa_xN/GaN HEMTs with Different Al Compositions

Yeo Jin Choi ¹, Jae-Hoon Lee ², Sung Jin An ¹ and Ki-Sik Im ^{3,*}

¹ Department of Advanced Materials Science and Engineering, Kumoh National Institute of Technology, Gumi 39177, Korea; dota23@kumoh.ac.kr (Y.J.C.); sungjinan@kumoh.ac.kr (S.J.A.)

² Yield Enhancement Team, Foundry, Samsung Electronics Company Ltd., Yongin 17113, Korea; jaehoon03.lee@samsung.com

³ Advanced Material Research Center, Kumoh National Institute of Technology, Gumi 39177, Korea

* Correspondence: ksim@kumoh.ac.kr

Received: 27 August 2020; Accepted: 15 September 2020; Published: 17 September 2020



Abstract: Al_xGa_{1-x}N/GaN heterostructures with two kinds of Al composition were grown by metal organic chemical vapor deposition (MOCVD) on sapphire substrates. The Al compositions in the AlGa_xN barrier layer were confirmed to be 13% and 28% using high resolution X-ray diffraction (HRXRD). Al_xGa_{1-x}N/GaN high-electron mobility transistors (HEMTs) with different Al compositions were fabricated, characterized, and compared using the Hall effect, direct current (DC), and low-frequency noise (LFN). The device with high Al composition (28%) showed improved sheet resistance (R_{sh}) due to enhanced carrier confinement and reduced gate leakage currents caused by increased Schottky barrier height (SBH). On the other hand, the reduced noise level and the low trap density (N_t) for the device of 13% of Al composition were obtained, which is attributed to the mitigated carrier density and decreased dislocation density in the Al_xGa_{1-x}N barrier layer according to the declined Al composition. In spite of the Al composition, the fabricated devices exhibited $1/f$ noise behavior with the carrier number fluctuation (CNF) model, which is proved by the curves of both (S_{Id}/I_d^2) versus $(g_m/I_d)^2$ and (S_{Id}/I_d^2) versus $(V_{gs}-V_{th})$. Although low Al composition is favorable to the reduced noise, it causes some problems like low R_{sh} and high gate leakage current. Therefore, the optimized Al composition in AlGa_xN/GaN HEMT is required to improve both noise and DC properties.

Keywords: GaN; AlGa_xN; HEMT; Al composition; low-frequency noise; carrier number fluctuation

1. Introduction

Al_xGa_{1-x}N/GaN high-electron mobility transistors (HEMTs) are very attractive devices for both high-power and high-temperature operations [1]. This is because the wide energy band gap (E_g) of above 3.4 eV allows for higher supply voltages and reliable device performances at high temperature [2]. In addition, spontaneous and piezoelectric polarization in the AlGa_xN/GaN heterostructures gives high electron densities and high transconductance (g_m), which lead to having advantages for applying high-frequency and high-current devices [3,4].

Generally, when Al composition in the Al_xGa_{1-x}N barrier layer increases, the conduction band discontinuity and the polarization-induced electrons are increased, which results in high sheet carrier concentration in the two-dimensional electron gas (2DEG) located at the Al_xGa_{1-x}N/GaN heterostructure [3]. However, high Al composition makes easy to generate the dislocations in the Al_xGa_{1-x}N barrier layer due to the large lattice mismatch between the Al_xGa_{1-x}N and GaN layers caused by the discrepancy of their E_g . These dislocations play the roles of trap states and charge scattering centers, which leads to the deterioration of device performance, such as severe current

collapse, increased gate leakage current, and degraded g_m [4]. Therefore, in order to achieve improved device performance, it is needed to optimize the Al composition in the $\text{Al}_x\text{Ga}_{1-x}\text{N}$ barrier layer.

Low-frequency noise (LFN) measurement for AlGaIn/GaN HEMTs is an efficient tool to examine device performance, analyze material defects, and study device reliability [5–8]. Many research groups have reported by investigating the effects of in situ/ex situ passivation layers [9,10], the gate-to-drain distance [7], and the types of GaN buffer layer [11] on the LFN of AlGaIn/GaN HEMTs. M. D. Hasan, et al. [6] demonstrated that the AlGaIn/GaN metal-oxide-semiconductor (MOS)-HEMT with Al composition of 20% exhibited a lower noise level than that of the device with Al composition of 35%. However, the noise fluctuations mechanism between the 2DEG channel and gate oxide in AlGaIn/GaN MOS-HEMTs are complicated due to their double gate oxide layers: (1) the AlGaIn barrier layer; (2) the deposited oxide layer. No detailed noise characterization has been performed in AlGaIn/GaN HEMT according to the Al composition without oxide layer. Here, we investigate the structural and electrical characteristics of $\text{Al}_x\text{Ga}_{1-x}\text{N}/\text{GaN}$ HEMTs with two different Al compositions ($x = 0.13$ and 0.28) using high resolution X-ray diffraction (HRXRD), the Hall effect, direct current (DC), and LFN measurement.

2. Materials and Methods

The $\text{Al}_x\text{Ga}_{1-x}\text{N}/\text{GaN}$ heterostructures were grown on sapphire substrates by metal organic chemical vapor deposition (MOCVD). The layer structure consisted of a 30 nm-thick GaN initial nucleation layer grown at low temperature, a 3 μm -thick highly resistive GaN buffer layer, and a AlGaIn barrier layer (Figure 1a). To find the Al composition and the thickness of AlGaIn, the ω -2 θ scan of the diffraction plane for two samples was measured using the HRXRD in Figure 1b. The detailed Al composition and AlGaIn thickness are shown in Table 1. The intensity of the GaN buffer layer was found to be sharp and high, but the AlGaIn peak located near the GaN peak presented to be broad and low (Figure 1b), which means that the GaN buffer layer exhibits much better crystal quality compared with the AlGaIn barrier layer. It was also noted that the AlGaIn peak shifts to positive as the AlGaIn composition increases. The reason for the peak shift is due to the decreased lattice constant of the AlGaIn barrier layer [12], which leads to the large lattice mismatch between the thin AlGaIn barrier layer and the underlying thick GaN layer. This results in generating the dislocations in the AlGaIn barrier layer as the Al composition increases [13]. Hall effect measurements showed that the sheet resistance (R_{sh}) for the $\text{Al}_x\text{Ga}_{1-x}\text{N}/\text{GaN}$ heterostructure with $x = 0.13$ and 0.28 were 1923 and 421 Ω/sq , respectively (the detailed electron mobilities and 2DEG densities for all samples are depicted in Table 1). The enhancement of R_{sh} as a function of the Al composition is due to the improved carrier confinement and polarization in the 2DEG quantum well [3].

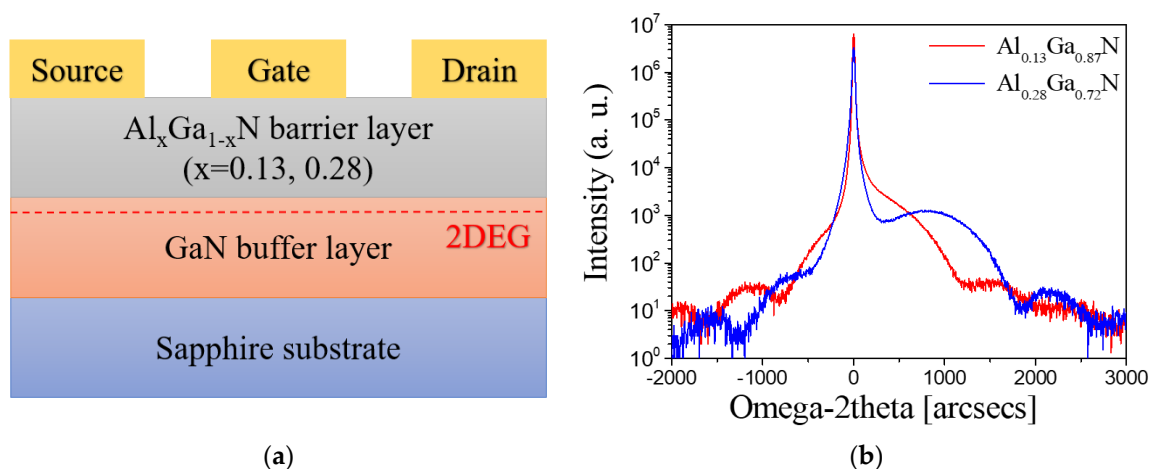


Figure 1. (a) Schematic cross-sectional view of the fabricated AlGaIn/GaN HEMTs; (b) High resolution X-ray diffraction (HRXRD) of symmetric (0002) ω -2 θ scan of AlGaIn/GaN heterostructures for different Al compositions.

Table 1. Structural parameters, sheet resistance, 2-dimensional electron gas (2DEG) densities, and electron mobility in Al_xGa_{1-x}N/GaN HEMTs measured by HRXRD and the Hall effect.

HRXRD		Hall Effect		
Al Composition [%]	AlGa _N Thickness [nm]	R _{sh} [Ω/sq]	μ [cm ² /V·s]	n _s [cm ⁻²]
13	20	1923	1200	0.27 × 10 ¹³
28	19	421	1380	1.07 × 10 ¹³

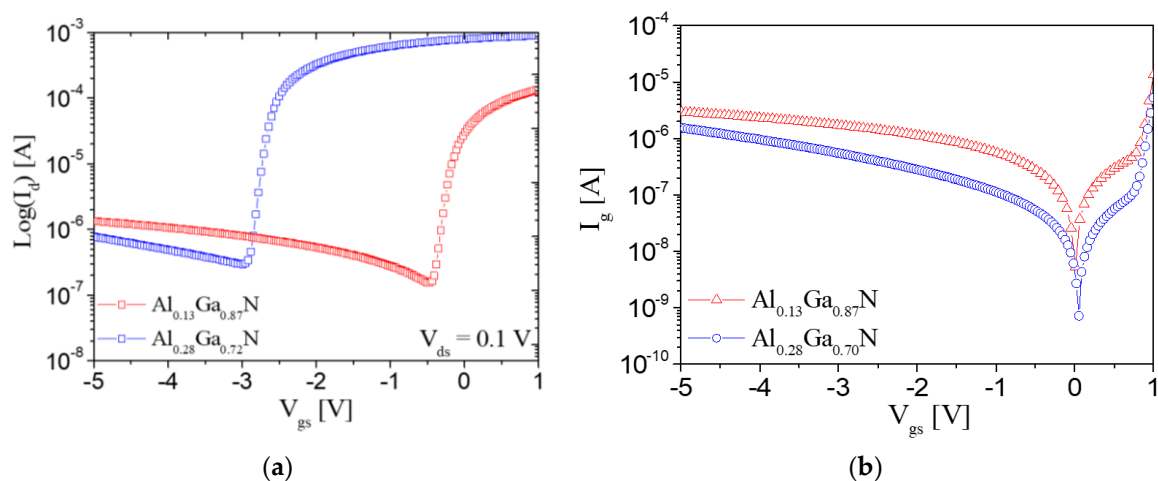
Device fabrication was commenced with mesa isolation by inductively coupled plasma-reactive ion etching (ICP-RIE). Ohmic contacts composed of Si/Ti/Al/Ni/Au (1/25/160/40/100 nm) were deposited and then were conducted by rapid thermal annealing at 850 °C for 30 s. Finally, the Ni/Au gate metal was deposited by e-beam evaporation. The fabricated AlGa_N/GaN HEMTs with two different compositions have a gate length (L_G) of 5 μm, a gate-source spacing (L_{CS}) of 5 μm, and a gate-drain spacing (L_{GD}) of 4 μm. The detailed device structure is illustrated in Figure 1a.

3. Results and Discussion

Figure 2 shows the logarithmic scale of drain current and gate leakage current of the fabricated Al_xGa_{1-x}N/GaN HEMTs. The threshold voltage (V_{th}) for two different Al compositions (x = 0.13 and 0.28) obtained using y-function ($= I_d / \sqrt{g_m}$) [14] are -0.17 and -2.7 V, respectively (Figure 2a). It is clearly observed that the gate leakage current decreases according to the raised Al composition, as shown in Figure 2b. The reason for the excellent leakage currents in the device with high Al composition is due to the enhanced Schottky barrier height (SBH) [3,15] caused by the enlargement of E_g of the AlGa_N barrier layer. From the I_g-V_{gs} curves in Figure 2b, the SBHs can be extracted using Equation (1) [16]:

$$I = I_0 \left[\exp\left(\frac{qV}{nkT}\right) - 1 \right] \text{ with } I_0 = AA^*T^2 \exp\left(\frac{-q\Phi_B}{kT}\right) \quad (1)$$

where I₀ is reverse saturation current, q is the electric charge, n is the ideality factor, kT is the thermal energy, Φ_B is the Schottky barrier height, A is the contact area, and A* is the effective Richardson constant. The SBHs, extracted from the intercept of the y-axis of the logarithmic plot of I/[1-exp(-qV/kT)] versus V, are 0.51 and 0.59 eV for the devices with Al composition of 13% and 28%, respectively.

**Figure 2.** (a) Drain current (logarithmic scale); (b) gate leakage current of AlGa_N/GaN HEMTs with different Al compositions.

LFN measurements were performed at room temperature by changing the gate bias from the subthreshold region to a strong accumulation region in the linear region (V_{ds} = 0.1 V). A fully

automatic LFN measurement system from Synergie Concept is used in the frequency ranges from 4 to 10³ Hz [17]. Figure 3a shows the drain current power spectral density (S_{Id}) for all devices at the same bias of $(V_{gs}-V_{th}) = 0.5$ V and $V_{ds} = 0.1$ V. The observed curves for all devices clearly exhibit 1/ f noise characteristics. When the Al concentration is high, the noise level becomes high, which is totally different with the gate leakage performances and R_{sh} properties. This behavior is attributed to the increased dislocations in the AlGa_xN barrier layer as a function of the Al composition due to the large lattice mismatch between the AlGa_xN and GaN layer.

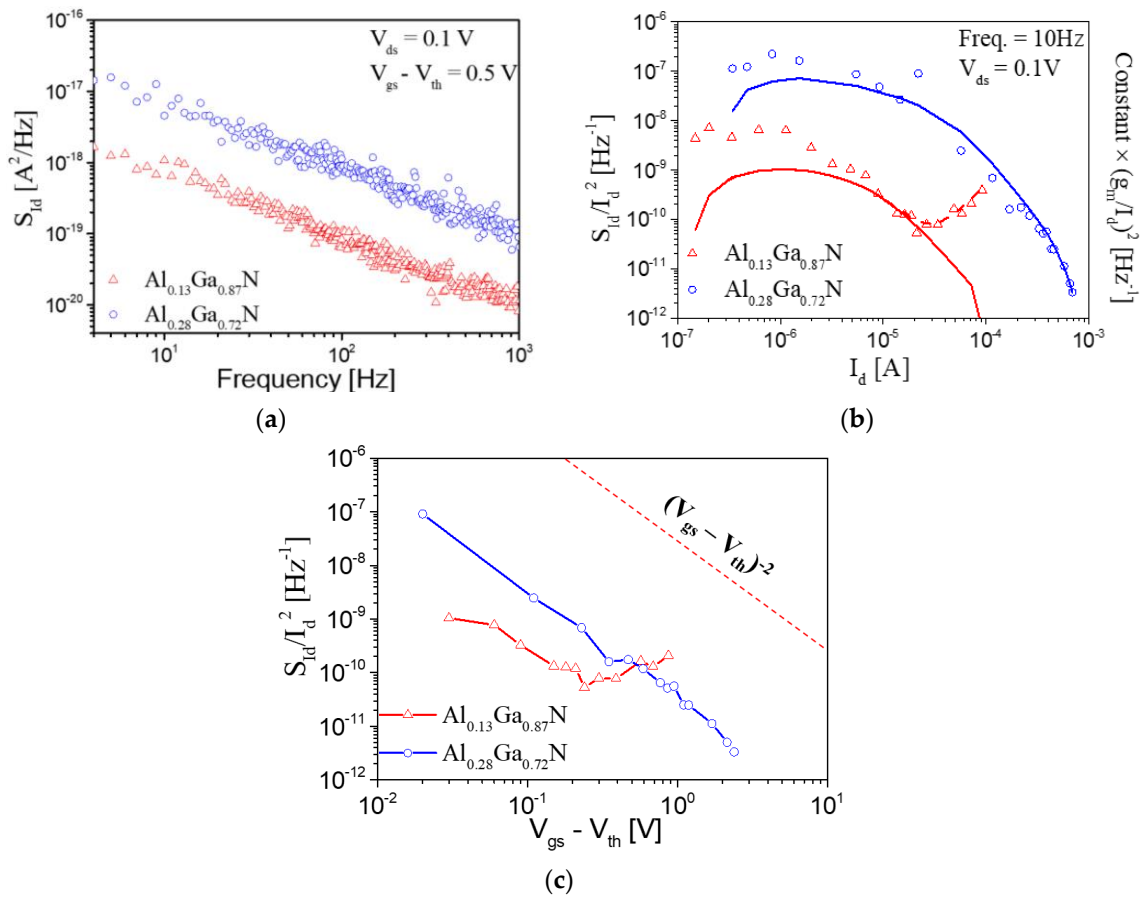


Figure 3. (a) S_{Id} versus frequency at the gate overdrive voltage $(V_{gs}-V_{th}) = 0.5$ V; (b) S_{Id}/I_d^2 (left scale) and $(\text{constant} \times (g_m/I_d)^2)$ (right scale) according to drain currents.; (c) dependence of S_{Id}/I_d^2 on $(V_{gs}-V_{th})$ in the device with the Al composition of 13% (red triangle) and 28% (blue circle), respectively. The corresponding solid lines in (b) show their $(g_m/I_d)^2$ for all devices and the red dashed line indicates $(g_m/I_d)^2 + S_{Rsd}(I_d/V_d)^2$ in Al_{0.13}Ga_{0.87}N HEMT ($V_{ds} = 0.1$ V and $f = 10$ Hz).

When the normalized S_{Id} (S_{Id}/I_d^2) matches with $(g_m/I_d)^2$, more informative results can be obtained using the following equations [18,19]:

$$\frac{S_{Id}}{I_d^2} = \left(\frac{g_m}{I_d}\right)^2 S_{Vfb} + S_{Rsd} \left(\frac{I_d}{V_d}\right)^2 \tag{2}$$

with

$$S_{Vfb} = \frac{q^2 k T \lambda N_t}{W L C_{ox}^2 f} \tag{3}$$

where S_{Rsd} is the spectral density of source-drain series resistance, S_{Vfb} is flat-band voltage fluctuations, λ is the oxide tunneling attenuation distance (≈ 0.11 nm) [20], N_t is the volumetric oxide trap density, WL is the channel area, C_{ox} is the gate dielectric capacitance per unit area, and f is frequency. As shown

in Figure 3b, the S_{Id}/I_d^2 of all devices investigated in this study is proportional to $(g_m/I_d)^2$. This indicates that the noise of AlGaN/GaN HEMTs is explained by the carrier number fluctuations (CNF) noise model, which shows that the origin of the noise is mainly due to the multiple trapping/de-trapping at the interface between the AlGaN barrier layer and the GaN channel. It is very interesting that the measured noise data in Al_{0.13}Ga_{0.87}N/GaN HEMT show the dependence of $\sim I_d^2$ at a relatively high drain current of 10^{-4} – 10^{-5} A. These increased noise values are believed to be due to mainly source/drain series resistance caused by the high R_{sh} of Al_{0.13}Ga_{0.87}N/GaN heterostructure, which is confined by Hall effect measurements. When considering the value of $S_{Rsd} = 5 \times 10^{-3} \Omega^2 \cdot \text{Hz}^{-1}$ using Equation (2), the S_{Id}/I_d^2 fit very well with CNF + source-drain resistance fluctuations (red dashed line in Figure 3b). Furthermore, a possible explanation is the increased gate leakage current at high drain current, as shown in Figure 2b, which is also responsible for increasing the noise value at high drain current [21].

In the CNF noise model, noise source in the fabricated devices originates from trapping/de-trapping into the shallow trap levels of the Al_xGa_{1-x}N barrier layer and/or the GaN buffer layer [8]. From Equation (2), the values of S_{Vfb} are calculated to be 4.0×10^{-12} and $8.5 \times 10^{-11} \text{ V}^2/\text{Hz}$ for the devices with Al composition of 13% and 28%, respectively. The corresponding N_t calculated using Equation (3) is 2.1×10^{18} and $4.9 \times 10^{18} \text{ cm}^{-3} \cdot \text{eV}^{-1}$, respectively. The Al_{0.28}Ga_{0.87}N/GaN HEMT exhibits the high N_t value, which is reflected by the trapping/de-trapping of many carriers due to the high carrier concentration in the AlGaN/GaN heterostructure and probably, the increased dislocation density of the AlGaN barrier layer as the Al composition increases [13].

Figure 3c shows the S_{Id}/I_d^2 according to the $(V_{gs}-V_{th})$ for all devices. All curves clearly show the slope of -2 for the S_{Id}/I_d^2 versus $(V_{gs}-V_{th})$. If the slope is -1 , the noise source is mainly from the Hooge mobility fluctuations (HMF) noise model [22]. These results also confirm that the fabricated devices follow the CNF noise model as a fluctuation mechanism [9,23].

4. Conclusions

AlGaN/GaN HEMTs with different Al compositions are fabricated and characterized through HRXRD, Hall effects, DC, and LFN measurements. The device with high composition shows improved R_{sh} and reduced gate leakage current. On the other hand, the noise levels and the calculated N_t are obtained to low values in Al_{0.13}Ga_{0.87}N/GaN HEMT. This is because the carrier density and dislocation density in the AlGaN barrier layer decrease as Al composition decreases. Regardless of the Al composition, the fabricated AlGaN/GaN HEMTs exhibit the $1/f^\gamma$ noise characteristics, with $\gamma = 1$ explained by the CNF noise model due to the carrier trapping/de-trapping at the AlGaN/GaN heterostructure. This noise mechanism is confirmed by the plotting of the curves of both (S_{Id}/I_d^2) versus $(g_m/I_d)^2$ and (S_{Id}/I_d^2) versus $(V_{gs}-V_{th})$. Both DC and noise performances can be improved by optimizing the Al composition and applying the additional deposition of the gate oxide layer.

Author Contributions: Writing—review and editing, Y.J.C., S.J.A., J.-H.L., and K.-S.I.; investigation, Y.J.C.; synthesis, J.-H.L.; fabrication, Y.J.C. and K.-S.I.; data collection of direct current (DC) and low-frequency noise (LFN), Y.J.C. and K.-S.I. All authors have read and agreed to the published version of the manuscript.

Funding: This work was supported by the National Research Foundation of Korea (NRF) funded by the Ministry of Education, Science and Technology (MEST) (No. NRF-2018R1A6A1A03025761, NRF-2019R1I1A1A01064011). This research was partially supported by Nano-Material Technology Development Program through the NRF funded by the Ministry of Science, ICT and Future Planning (2009-0082580).

Conflicts of Interest: The authors declare no conflict of interest.

References

1. Arulkumaran, S.; Egawa, T.; Ishikawa, H.; Jimbo, T. Characterization of different-Al-content Al_xGa_{1-x}N/GaN heterostructures and high-electron-mobility transistors on sapphire. *IEEE Electron Device Lett.* **2003**, *21*, 888. [[CrossRef](#)]
2. Nanjo, T.; Takeuchi, M.; Suita, M.; Oishi, T.; Abe, Y.; Tokuda, Y.; Aoyagi, Y. Remarkable breakdown voltage enhancement in AlGa_N channel high electron mobility transistors. *Appl. Phys. Lett.* **2008**, *92*, 263502. [[CrossRef](#)]
3. Ambacher, O.; Foutz, B.; Smart, J.; Shealy, J.; Weimann, N.G.; Chu, K.; Murphy, M.; Sierakowski, A.J.; Schaff, W.J.; Eastman, L.F.; et al. Two dimensional electron gases induced by spontaneous and piezoelectric polarization in undoped and doped AlGa_N/Ga_N heterostructures. *J. Appl. Phys.* **2000**, *87*, 334–344. [[CrossRef](#)]
4. Disanto, D.W.; Sun, H.F.; Bolognesi, C.R. Ozone passivation of slow transient current collapse in AlGa_N/Ga_N field-effect transistors: The role of threading dislocations and the passivation mechanism. *Appl. Phys. Lett.* **2006**, *88*, 013504. [[CrossRef](#)]
5. Sai, P.O.; Jorudas, J.; Dub, M.; Sakowicz, M.; Jakštas, V.; But, D.B.; Prystawko, P.; Cywiński, G.; Kašalynas, I.; Knap, W.; et al. Low frequency noise and trap density in Ga_N/AlGa_N field effect transistors. *Appl. Phys. Lett.* **2019**, *115*, 183501. [[CrossRef](#)]
6. Hasan, R.; Motayed, A.; Fahad, S.; Rao, M.V. Fabrication and comparative study of DC and low frequency noise characterization of Ga_N/AlGa_N based MOS-HEMT and HEMT. *J. Vac. Sci. Technol. B* **2017**, *35*, 052202. [[CrossRef](#)]
7. Rzin, M.; Routoure, J.-M.; Guillet, B.; Méchin, L.; Morales, M.; Lacam, C.; Gamarra, P.; Ruterana, P.; Medjdoub, F. Impact of Gate–Drain Spacing on Low-Frequency Noise Performance of In Situ Si_N Passivated InAlGa_N/Ga_N MIS-HEMTs. *IEEE Trans. Electron Devices* **2017**, *64*, 2820–2825. [[CrossRef](#)]
8. McWhorter, A.L. *1/f Noise and Germanium Surface Properties in Semiconductor Surface Physics*; University of Pennsylvania Press: Philadelphia, PA, USA, 1957; pp. 207–208.
9. Rzin, M.; Guillet, B.; Méchin, L.; Gamarra, P.; Lacam, C.; Medjdoub, F.; Routoure, J.-M. Impact of the in situ Si_N Thickness on Low-Frequency Noise in MOVPE InAlGa_N/Ga_N HEMTs. *IEEE Trans. Electron Devices* **2019**, *66*, 5080–5083. [[CrossRef](#)]
10. Do, T.N.T.; Malmros, A.; Gamarra, P.; Lacam, C.; di Forte-Poisson, M.-A.; Tordjman, M.; Hörberg, M.; Aubry, R.; Rorsman, N.; Kuylenstierna, D. Effects of Surface Passivation and Deposition Methods on the 1/f Noise Performance of AlIn_N/AlN/Ga_N High Electron Mobility Transistors. *IEEE Electron Device Lett.* **2015**, *36*, 315–317. [[CrossRef](#)]
11. Im, K.-S.; Choi, J.S.; Hwang, Y.M.; An, S.J.; Roh, J.-S.; Kang, S.-H.; Lee, J.-H.; Lee, J.H.; Lee, J.H. 1/f noise characteristics of AlGa_N/Ga_N HEMTs with periodically carbondoped Ga_N buffer layer. *Microelectron. Eng.* **2019**, *215*, 110985. [[CrossRef](#)]
12. Loganathan, R.; Jayasakthi, M.; Prabakaran, K.; Ramesh, R.; Arivazhagan, P.; Baskar, K. Studies on dislocation and surface morphology of Al_xGa_{1-x}N/GaN heterostructures grown by MOCVD. *J. Alloys Compd.* **2014**, *616*, 363–371. [[CrossRef](#)]
13. Jayasakthi, M.; Ramesh, R.; Arivazhagan, P.; Loganathan, R.; Prabakaran, K.; Balaji, M.; Baskar, K. Structural and optical characterization of AlGa_N/Ga_N layers. *J. Cryst. Growth* **2014**, *401*, 527–531. [[CrossRef](#)]
14. Ghibaudo, G. New method for the extraction of MOSFET parameters. *Electron. Lett.* **1988**, *24*, 543. [[CrossRef](#)]
15. Fieger, M.; Eickelkamp, M.; Koshroo, L.R.; Dikme, Y.; Nocolak, A.; Kalisch, H.; Heuken, M.; Jansen, R.; Vescan, A. MOVPE, processing and characterization of AlGa_N/Ga_N HEMTs with different Al concentrations on silicon substrates. *J. Cryst. Growth* **2007**, *298*, 843–847. [[CrossRef](#)]
16. Ravinandan, M.; Rao, P.K.; Reddy, V.R. Analysis of the current–voltage characteristics of the Pd/Au Schottky structure on n-type Ga_N in a wide temperature range. *Semicond. Sci. Technol.* **2009**, *24*, 035004. [[CrossRef](#)]
17. Chroboczek, J.A.; Piantino, G. Low Noise Current Amplifier with Programmable Gain and Polarization for Use in Electrical Measurement of Semiconductor Circuits, such as Transistors, with the Circuit Being Low Noise and Having a Protection Circuit for the Input. France Patent No. 15075, 22 November 2000.
18. Ghibaudo, G.; Roux, O.; Nguyen-Duc, C.; Balestra, F.; Brini, J. Improved Analysis of Low Frequency Noise in Field-Effect MOS Transistors. *Phys. Status Solidi A* **1991**, *124*, 571–581. [[CrossRef](#)]
19. Ghibaudo, G.; Boutchacha, T. Electrical noise and RTS fluctuations in advanced CMOS devices. *Microelectron. Reliab.* **2002**, *42*, 573–582. [[CrossRef](#)]

20. Im, K.-S.; An, S.J.; Theodorou, C.G.; Ghibaudo, G.; Cristoloveanu, S.; Lee, J.-H. Effect of Gate Structure on the Trapping Behavior of GaN Junctionless FinFETs. *IEEE Electron Device Lett.* **2020**, *41*, 832–835. [[CrossRef](#)]
21. Pala, N.; Gaska, R.; Romyantsev, S.; Shur, M.; Khan, M.A.; Hu, X.; Simin, G.; Yang, J. Low-frequency noise in AlGaIn/GaN MOS-HFETs. *Electron. Lett.* **2000**, *36*, 268. [[CrossRef](#)]
22. Peransin, J.-M.; Vignaud, P.; Rigaud, D.; Vandamme, L.K.J. 1/f noise in MODFETs at low drain bias. *IEEE Trans. Electron Devices* **1990**, *37*, 2250–2253. [[CrossRef](#)]
23. Romyantsev, S.L.; Deng, Y.; Shur, S.; Levinshtein, M.E.; Khan, M.A.; Simin, G.; Yang, J.; Hu, X.; Gaska, R. On the low frequency noise mechanisms in GaN/AlGaIn HFETs. *Semicond. Sci. Technol.* **2003**, *18*, 589–593. [[CrossRef](#)]



© 2020 by the authors. Licensee MDPI, Basel, Switzerland. This article is an open access article distributed under the terms and conditions of the Creative Commons Attribution (CC BY) license (<http://creativecommons.org/licenses/by/4.0/>).